Complex Permittivity of Water as a Function of Frequency and Temperature

Udo Kaatze

Drittes Physikalisches Institut, Universität Göttingen, Bürgerstrasse 42-44, D-3400 Göttingen, West Germany

Sets of complex permittivity values for pure water are presented for nine temperatures between 0 and 50 °C and for microwave frequencies from 1.1 to 57 GHz. The data are analyzed together with static permittivity values and many sporadic microwave data found in the published literature. At all temperatures considered in this analysis (-4.1 °C $\leq$ T $\leq$ 60 °C) the frequency-dependent complex permittivities can be well described by a Debye-type relaxation spectral function reflecting one discrete relaxation time. The parameter values for this function as obtained by a nonlinear regression analysis of the measured dielectric spectra are displayed in tabular format. Also given are empirical correlations allowing these parameters to be interpolated with respect to the temperature.

Introduction

The insight into the molecular properties of water has a substantial influence on ecological, industrial, and medical developments. This unique liquid therefore plays a dominant role in many fields of scientific research. Our increasing interest, of course, is not only directed toward the unsolved mysteries of pure water itself. Considerable effort is undertaken to elucidate the molecular structure and dynamics of solutions, both electrolytic and biomolecular. A fundamental precondition for many studies of aqueous systems is the precise knowledge of the pure solvent properties. Water is also a most suited reference liquid in calibration and test measurement.

The complex (electric) permittivity

$$\epsilon(\nu,T) = \epsilon'(\nu,T) - i\epsilon''(\nu,T) \qquad (1)$$

measured as a function of frequency ν and temperature T is of interest for various reasons. It shows how the liquid responds to electromagnetic waves, one of our most important means of communications. In addition, the microwave part of the dielectric spectrum presents distinct dispersion ($d\epsilon'(\nu,T)/d\nu < 0$) and absorption ($\epsilon''(\nu,T) > 0$) characteristics. These are due to restricted orientational motions of water molecules. Measurements of the permittivity of aqueous systems as a function of frequency and temperature enable conclusions on relevant molecular interactions and arrangements.

Because of the importance of the permittivity of water in many fields of interest, the available data had been collected and critically evaluated some years ago (1). That review, however, aimed at the correct analytical description of the water spectrum by a physically meaningful relaxation function rather than a compilation of experimental results. In various applications there is an additional demand for original data. These are given in this article. Besides the previous results from this laboratory, recently measured permittivity data at further temperatures are also displayed. Empirical correlations are presented which allow for the interpolation with respect to both frequency and temperature. Literature data are referenced and included in the analysis.

Experimental Methods

The water was bidistilled and deionized by bed ion exchange. Its specific electric dc conductivity σ was smaller than 2×10^{-4} S/m. Contributions $\sigma/(\epsilon_0\omega)$ to the ϵ'' values are thus negligibly small ($\epsilon_0 = 8.854 \times 10^{-12}$ A s V^{-1} m^{-1}; $\omega = 2\pi\nu$).

Spot frequency measurements have been performed by using a traveling-wave technique as first proposed by Buchanan (2) and later on improved by Pottel (3). As schematically shown by Figure 1, a propagating electromagnetic wave transmitted through an appropriate specimen cell of variable thickness was probed interferometrically. We used cells (6 in Figure 1) that essentially consist of a piece of circular cylindrical waveguide or coaxial line. It was sealed against the feeding line by a window (7) made of Teflon, silicone rubber, or ceramic dielectrics. A receiving probe (8), also a circular waveguide or coaxial line, was immersed in the liquid. Provided with high-precision ball bush guides this probe was shiftable free of backlash along the direction z of wave propagation.

At a suitable starting position $z = s_n$ of the probe the reference wave of the double-beam interferometer was adjusted so that the probe signal and the reference signal interfered to zero. The reference branch contained a phase shifter (9) and a microwave attenuator (10) for this purpose. It was additionally provided with a calibrated attenuator (11), the phase shift of which was constant. When the probe was moved for the wavelength λ and the calibrated attenuator was adjusted for the attenuation per wavelength, $\alpha\lambda$, zero signal was again obtained.

The permittivity of the sample liquid is related to the measured quantities ν, λ, and $\alpha\lambda$ according to the equations

$$\epsilon'(\nu) = \left[\frac{\lambda_0}{\lambda}\right]^2 - \left[\frac{\alpha\lambda_0}{2\pi}\right]^2 + \left[\frac{\lambda_0}{\lambda_c}\right]^2 \qquad (2)$$

$$\epsilon''(\nu) = \frac{\alpha\lambda_0^2}{\pi\lambda} \qquad (3)$$

where λ_0 = (speed of light)/ν denotes the wavelength of free space and λ_c the cutoff wavelength of the empty cell.

Seven double-beam interferometers, each matched to a limited frequency range were used. One was constructed with coaxial line components, and the others were constructed with standard waveguide devices. For reasons of comparison at least two different cells and two different calibrated attenuators were available for each interferometer. All cells were surrounded by a coat for circulating thermostat fluid to enable the temperature of the sample to be controlled to within ±0.05 K.

Uncertainty of Primary Data

Precision. High stability in both the mechanical and electronic components of the interferometers together with a sufficiently effective temperature control and a very sensitive superheterodyne zero signal detection allowed for an adequate reproducibility in the measurements at all frequencies below 26 GHz. An example for the precision of repeatedly measured data is shown in Figure 2. The spread in the values λ_n ($n = 1, ..., 17$) for the wavelength within the liquid is smaller than ±0.1% in this case. In the values $(\alpha\lambda)_n$ of the attenuation per wavelength the spread is smaller than 0.3%. Due to the higher $\alpha\lambda$ values at concurrently reduced receiver sensitivity, the measurements were less reproducible above 26 GHz. At 40 GHz, for instance, the scatter is ±2% in both the λ_n and $(\alpha\lambda)_n$ values.
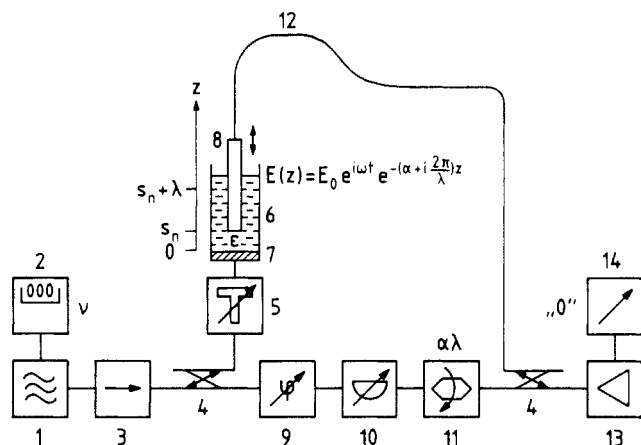
Figure 1. Schematic representation of the microwave double-beam interferometers. 1, monochromatic oscillator; 2, frequency counter or frequency meter; 3, uniline or coaxial attenuator; 4, directional coupler or coaxial beam splitter; 5, impedance matching transformer; 6, sample cell with 7, dielectric window, and 8, precisely shiftable probe; 9, phase shifter; 10, variable attenuator; 11, calibrated variable attenuator with constant phase shift; 12, flexible waveguide or coaxial line; 13, superheterodyne receiver; 14, zero signal indicator.
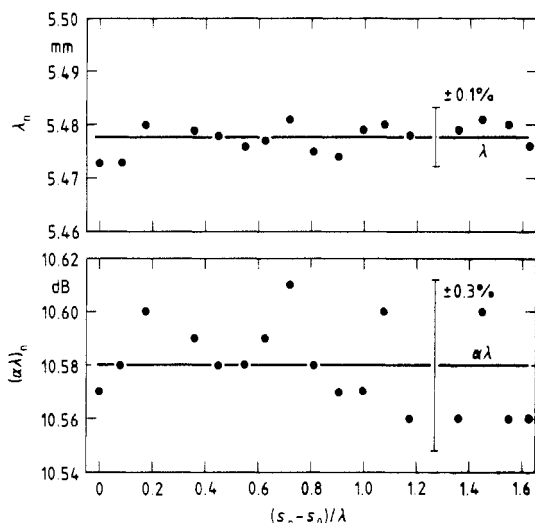

Figure 2. Single values at 6.457 GHz of the wavelength λ_n and attenuation per wavelength, $(\alpha\lambda)_n$, for water at 15 °C plotted as a function of the starting position s_n (n = 1, ..., 17) of the probe. Also shown are the mean values λ and $\alpha\lambda$, respectively, as well as bars indicating the range of scatter in the data.

Accuracy. The frequency was determined and kept constant during the measurements with a negligibly small error. Likewise precisely known was the position z of the probe within the liquid. Remaining sources of possible systematic errors were (a) small deviations from completely coaxial movements of the probe, (b) contributions from multiply reflected signals, (c) the presence of higher order field modes within the sample, and (d) imperfections of the calibrated attenuators either in the reading of the adjusted attenuation or in the invariability of the phase shift.

If one of the three first effects acts as a noticeable influence on the measurements, the λ_n and $(\alpha\lambda)_n$ values should characteristically depend on the starting positions s_n of the probe. As demonstrated by Figure 2, this was obviously not the case. In addition to this test, differently constructed specimen cells have been used in each frequency band to look for possible influences from sources a-c. No systematic errors exceeding the limits of reproducibility of the data have been found thereby.

Imperfections of the calibrated attenuators have been considered by using different devices (up to four) in each frequency band and also by analyzing how well adjoining data measured
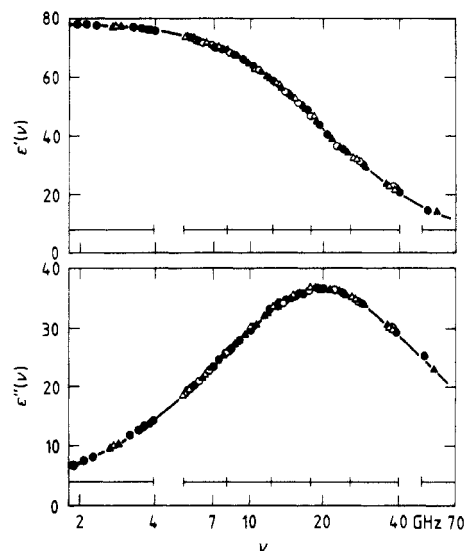
Figure 3. Real part, ϵ', and negative imaginary part, ϵ'', of the complex permittivity displayed as a function of frequency ν for water at 25 °C. Different figure symbols indicate different runs of measurements. Between these runs either the specimen cells or the calibrated attenuators of the microwave interferometers have been exchanged. Also shown by bars is the effective frequency band for each interferometer.

Table I. Experimental Uncertainties of the Complex Permittivity Values for Pure Water; Effects of Possible Systematic Errors Included

ν, GHz	$\Delta\epsilon'/\epsilon'$, %	$\Delta\epsilon''/\epsilon''$, %
1.1–5.3	1	3
5.3–12.5	1	1
12.5–18	1.5	1
18–26	2	1
26–30	2.5	2
30–40	4	3
40–57	10	4

with different interferometers are matched. As shown by Figure 3, this has been done in great detail at 25 °C. As a result of this analysis, the errors given in Table I were found.

Results and Semiempirical Representation of Data

In Table II the primary complex permittivity data from this laboratory are compiled as a function of frequency and temperature. The data have been analyzed together with previously published microwave (2, 9–42) and static (43, 44) permittivity values. It was found that the dielectric spectra can be sufficiently well represented by a Debye-type relaxation function. As has been realized previously (45), this is also true if far-infrared data are included in the analysis. The Debye function (46) is given by the relation

$$\epsilon(\nu) = \epsilon(\infty) + \frac{\epsilon(0) - \epsilon(\infty)}{1 + i\omega\tau} \tag{4}$$

To show that the measured spectra are compatible with this function, the permittivity values at microwave frequencies for water at 20 °C are displayed in an $\epsilon'(\nu)$ versus $\nu\epsilon''(\nu)$ plot in Figure 4. As predicted by eq 4, a straight line is defined by the data.

Equation 4 has been fitted to the sets of measured permittivity values by a nonlinear least-squares regression analysis causing the variance

$$V = \frac{1}{N_{\epsilon'} - 1}\sum_{n=1}^{N_{\epsilon'}} [W_{\epsilon'}(\nu_n)(\epsilon'_{measd}(\nu_n) - \epsilon'_{calcd}(\nu_n))] +$$

$$\frac{1}{N_{\epsilon''} - 1}\sum_{n=1}^{N_{\epsilon''}} [W_{\epsilon''}(\nu_n)(\epsilon''_{measd}(\nu_n) - \epsilon''_{calcd}(\nu_n))] \tag{5}$$

Table II. Complex Permittivity Data for Water as a Function of Frequency and Temperature

ν, GHz	ε'(ν)	ε''(ν)	ν, GHz	ε'(ν)	ε''(ν)	ν, GHz	ε'(ν)	ε''(ν)	ν, GHz	ε'(ν)	ε''(ν)
					0 °C (4)						
5.305	66.7	35.6	7.688	53.6	40.3	15.15	28.2	36.1	26.83	15.0	25.2
6.565	59.5	38.8	12.56	33.9	38.6	17.40	23.9	33.5	36.55	11.1	19.9
					5 °C (5)						
1.150	85.1	8.56	3.723	76.0	24.6	12.82	38.9	39.2	26.49	17.7	28.0
1.800	83.7	13.2	5.345	69.8	31.8	15.06	33.6	37.1	37.94	12.5	21.3
2.786	80.8	19.5	7.762	58.6	37.8	17.35	28.1	35.8			
					10 °C						
3.376	79.6	19.2	7.889	62.1	34.7	15.04	37.9	38.5	29.08	19.4	28.2
5.368	71.8	27.9	8.780	58.1	35.9	16.59	34.6	38.3	38.41	14.2	23.9
6.462	67.8	31.2	13.50	41.8	38.7	26.97	21.2	30.8			
					15 °C						
3.151	79.0	16.0	7.660	65.5	31.1	15.39	41.6	37.6	26.80	25.2	32.5
3.901	77.0	19.2	10.25	57.0	35.5	17.80	36.8	37.4	36.44	17.9	26.5
5.497	72.5	24.7	11.59	52.4	37.1	24.23	26.8	33.5	39.73	16.4	25.1
6.457	69.7	27.9	13.36	47.8	37.7						
					20 °C (6)						
1.594	79.8	7.39	3.137	78.4	13.9	7.703	67.4	28.2	17.31	42.0	37.1
1.914	79.8	8.41	3.843	76.7	16.6	12.47	53.6	35.5	26.65	26.5	33.9
2.176	78.9	9.32	5.424	73.3	21.9	14.77	47.9	36.9	36.56	17.6	28.8
2.214	79.1	10.3	6.412	70.9	25.0						
					25 °C (1)						
1.821	78.0	6.49	6.300	71.2	21.6	11.73	58.5	32.3	19.02	41.7	36.2
2.000	77.9	7.57	6.414	70.9	22.1	12.00	58.2	33.1	21.01	38.0	36.3
2.200	77.5	8.22	6.729	70.3	22.7	12.49	56.6	33.4	23.53	34.4	35.8
2.610	76.9	9.77	6.850	69.7	23.0	12.50	56.6	33.3	24.45	32.8	35.2
2.628	77.1	9.86	6.958	69.7	23.3	12.53	56.6	33.4	26.43	31.1	34.8
2.800	76.6	10.6	7.267	69.2	24.2	12.77	55.8	33.5	26.64	30.8	34.6
3.417	76.4	12.9	7.406	68.8	24.5	13.14	55.3	34.2	26.70	31.0	34.6
3.623	75.8	13.4	7.681	68.7	25.3	13.38	54.0	34.0	26.79	30.0	34.3
3.733	75.3	14.5	7.850	67.9	25.6	13.82	53.5	34.5	26.83	31.0	34.9
3.750	75.6	13.7	7.900	67.8	25.7	14.23	52.6	34.7	27.61	29.9	34.1
3.922	75.7	14.3	7.941	67.8	25.8	15.24	50.0	35.3	28.13	29.4	34.1
5.300	73.1	18.7	7.950	67.6	25.7	15.63	49.6	35.8	28.58	29.2	33.9
5.306	73.1	18.7	8.244	67.1	26.0	16.14	48.2	35.5	36.56	21.4	30.1
5.433	73.1	19.3	8.579	66.8	27.2	16.60	47.0	35.9	36.84	21.3	30.0
5.536	72.7	19.4	8.979	65.4	27.7	17.17	45.4	36.1	37.81	21.1	29.6
5.638	72.6	19.8	9.516	63.8	28.7	17.38	45.5	36.4	37.97	20.8	29.5
5.853	72.3	20.4	10.23	62.0	30.0	17.43	45.6	36.1	39.62	20.6	29.1
6.000	71.9	20.6	10.45	61.1	30.2	18.02	44.4	36.7	52.25	15.3	23.9
6.145	71.5	21.1	11.32	59.5	31.8	18.48	42.7	36.6	57.78	11.5	22.5
					30 °C						
3.146	75.3	10.1	7.318	69.3	21.9	13.43	56.4	31.7	17.67	48.4	34.8
3.515	74.9	11.3	7.738	68.8	22.7	15.00	53.1	32.9	26.75	34.8	34.6
3.922	74.4	12.4	8.508	67.2	24.2	15.15	53.1	33.1	28.78	32.7	34.2
5.345	72.7	16.3	10.02	64.2	26.8	16.54	50.5	34.3	28.85	33.2	33.8
6.004	71.6	18.5	12.64	58.4	31.1	17.44	48.6	34.6	39.01	23.7	29.7
6.828	70.5	20.7									
					35 °C (7)						
5.340	71.7	14.6	12.47	60.3	28.1	26.84	36.7	34.6	36.53	26.3	31.8
7.738	68.4	20.3	17.45	51.2	32.6						
					50 °C (8)						
7.707	67.2	14.5	17.46	56.3	27.2	26.78	44.2	32.0	36.30	34.3	32.6
12.47	61.5	21.4									

to adopt its absolute minimum. $N_{\epsilon'}$ and $N_{\epsilon''}$ denote the number of ϵ' and ϵ'' values, respectively. The weighing factors $W_{\epsilon'}(\nu_n)$ and $W_{\epsilon''}(\nu_n)$ have been calculated according to the relations

$$W_{\epsilon'}(\nu_n) = \frac{\epsilon'_{measd}(\nu_n)/\Delta\epsilon'(\nu_n)}{\sum\limits_{n=1}^{N_{\epsilon'}} \epsilon'_{measd}(\nu_n)/\Delta\epsilon'(\nu_n)} \tag{6}$$

and

$$W_{\epsilon''}(\nu_n) = \frac{\epsilon''_{measd}(\nu_n)/\Delta\epsilon''(\nu_n)}{\sum\limits_{n=1}^{N_{\epsilon''}} \epsilon''_{measd}(\nu_n)/\Delta\epsilon''(\nu_n)} \tag{7}$$

using the experimental errors given in Table I or quoted by the

authors of literature data, respectively. The values obtained by this fitting procedure for the low-frequency permittivity $\epsilon(0)$, the extrapolated high-frequency permittivity $\epsilon(\infty)$, and the relaxation time τ are collected in Table III. Also included in this table are some data at temperatures at which we have published experimental permittivity values only (1).

The dependence of these parameters upon the temperature T can be empirically described by the expressions

$$\epsilon(0) = 10^{(1.94404-1.991\times10^{-3} \text{ K}^{-1}(T-273.15 \text{ K}))} \tag{8}$$

$$\epsilon(\infty) = 5.77 - 2.74 \times 10^{-2} \text{ K}^{-1}(T - 273.15 \text{ K}) \tag{9}$$

$$\tau = (3.745 \times 10^{-15} \text{ s})(1 + (7 \times 10^{-5} \text{ K}^{-2}) \times (T- 300.65 \text{ K})^2) \exp((2.2957 \times 10^3 \text{ K})/T) \tag{10}$$
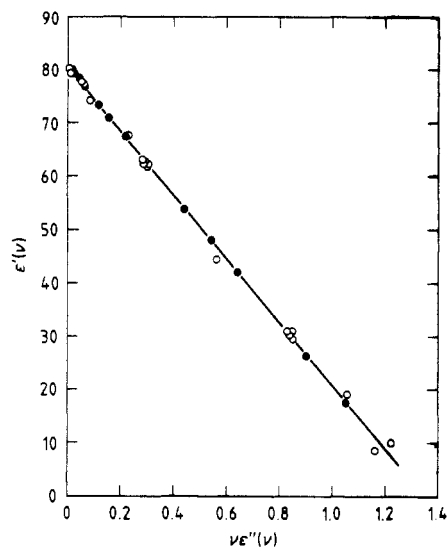
Figure 4. Plot of ϵ' versus $\nu\epsilon''$ for water at 20 °C. Full circles represent data from this laboratory (Table II), open circles represent data from the published literature (2, 10-14, 18, 19, 21, 23, 25, 27, 30, 33, 34, 37, 42).
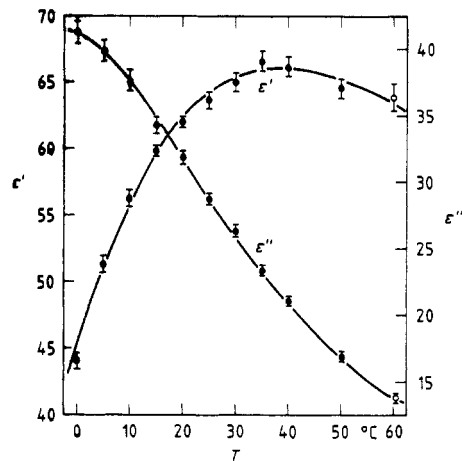
Figure 5. Real part, ϵ', and negative imaginary part, ϵ'', of the complex permittivity of water at 9.375 GHz shown as a function of temperature T. The full curves represent the predictions of the empirical relations 8-10 and 4. The experimental data have been taken from the literature (●, ref 2; O, 9.346 GHz (11)).

Relation 8 was originally derived for static permittivity values measured between 500 Hz and 100 kHz (44). In this paper the high-frequency permittivity is just defined to allow for the interpolation of the permittivity values below 100 GHz. The $\epsilon(\infty)$ values inferred from the microwave data are less reliable with respect to the far-infrared properties of water. The high-frequency permittivity values, for instance, change for a small amount, if measured data of the near-millimeter-wavelength region are included in the analysis (45). Such changes are indeed of minor importance for the predictions at microwave frequencies but might be relevant in the discussion of the water spectrum above 100 GHz. Moreover, the use of the Debye function (eq 4) in the extrapolation to high frequencies has to be questioned, for this relaxation function corresponds to an exponential dielectric decay function that cannot correctly account for the short-time behavior of the electric polarization.

At frequencies below 100 GHz and temperatures between -4.1 and 60 °C relations 8-10 together with eq 4 can be used to calculate the complex permittivity $\epsilon(\nu,T)$ within the present limits of experimental errors. An example is given in Figure 5, where the predictions of the empirical functions are compared

Table III. Parameters of the Debye Relaxation Spectral Function (Eq 4) for Water at Various Temperatures

T, °C	$\epsilon(0) \pm \Delta\epsilon(0)$	$\epsilon(\infty) \pm \Delta\epsilon(\infty)$	$\tau \pm \Delta\tau$, ps
-4.1	89.25 ± 0.2	5.9 ± 0.3	21.10 ± 0.2
0	87.91 ± 0.2	5.7 ± 0.2	17.67 ± 0.1
5	85.83 ± 0.2	5.7 ± 0.2	14.91 ± 0.1
10	83.92 ± 0.2	5.5 ± 0.2	12.68 ± 0.1
15	82.05 ± 0.2	6.0 ± 0.5	10.83 ± 0.2
20	80.21 ● 0.2	5.6 ± 0.2	9.36 ± 0.05
25	78.36 ± 0.05	5.2 ± 0.1	8.27 ± 0.02
30	76.56 ± 0.2	5.2 ± 0.4	7.28 ± 0.05
35	74.87 ± 0.2	5.1 ± 0.3	6.50 ± 0.05
40	73.18 ± 0.2	3.9 ± 0.3	5.82 ± 0.05
50	69.89 ± 0.2	4.0 ± 0.3	4.75 ± 0.05
60	66.70 ± 0.2	4.2 ± 0.3	4.01 ± 0.05

with previously published experimental data.

Literature Cited

(1) Kaatze, U.; Uhlendorf, V. Z. Phys. Chem. (Munich) 1981, 126, 151.
(2) Buchanan, T. J. Proc. Inst. Electr. Eng., Part 3 1952, 99, 61.
(3) Pottel, R. Ber. Bunsen-Ges. Phys. Chem. 1965, 69, 363.
(4) Gottlob, D. Diplom-Thesis, University of Göttingen, 1969.
(5) Lossen, O. Diplom-Thesis, University of Göttingen, 1966.
(6) Müller, S. C. Diplom-Thesis, University of Göttingen, 1975.
(7) Adolph, D. Diplom-Thesis, University of Göttingen, 1969.
(8) Giese, K. Diplom-Thesis, University of Göttingen, 1964.
(9) Conner, W. P.; Smyth, C. P. J. Am. Chem. Soc. 1943, 65, 382.
(10) Lane, J. A.; Saxton, J. A.; Meteorological Factors in Radio-Wave Propagation; The Physical Society: London, 1946.
(11) Collie, C. H.; Hasted, J. B.; Ritson, D. M. Proc. Phys. Soc., London 1948, 60, 145.
(12) Cook, H. F. Br. J. Appl. Phys. 1952, 3, 249.
(13) Lane, J. A.; Saxton, J. A. Proc. R. Soc. London, Ser. A 1952, 213, 400.
(14) Hasted, J. B.; El-Sabeh, S. H. M. Trans. Faraday Soc. 1953, 49, 1003.
(15) Little, V. I. Proc. Phys. Soc., London, Ser. B 1953, 66, 175.
(16) Hertel, P.; Stralton, A. W.; Tolbert, C. W. J. Appl. Phys. 1953, 24, 956.
(17) Poley, J. Ph. Appl. Sci. Res., Ser. B 1955, 4, 337.
(18) Grant, E. H.; Buchanan, T. J.; Cook, H. F. J. Chem. Phys. 1957, 26, 156.
(19) Rampolla, R. W.; Miller, R. C.; Smyth, C. P. J. Chem. Phys. 1959, 30, 566.
(20) Grant, E. H. Br. J. Appl. Phys. 1959, 10, 87.
(21) Sandus, O.; Lubitz, B. J. Phys. Chem. 1961, 65, 881.
(22) Weiss, E.; Gerdes, E.; Hoffmann, H.-J. Z. Phys. Chem. (Leipzig) 1965, 228, 51.
(23) Grant, E. H.; Shack, R. Br. J. Appl. Phys. 1967, 18, 1807.
(24) Barthel, J.; Schmithals, F.; Behret, H. Z. Phys. Chem. (Munich) 1970, 71, 115.
(25) Vial, J. M. Thèse de troisième cycle, University of Bordeaux, 1971.
(26) Sheppard, R. J. J. Phys. D 1972, 5, 1576.
(27) Bottreau, A.-M.; Marzat, C.; Lacroix, Y.; Dutuit, Y. C. R. Acad. Sci., Ser. B 1973, 276, 255.
(28) Kaatze, U. Appl. Phys. 1973, 2, 241.
(29) Van Loon, R.; Finsy, R. Rev. Sci. Instrum. 1973, 44, 1204.
(30) Delbos, G. Rev. Phys. Appl. 1974, 9, 967.
(31) Grant, E. H.; Sheppard, R. J. J. Chem. Phys. 1974, 60, 1792.
(32) Hallenga, K. Rev. Sci. Instrum. 1975, 46, 1691.
(33) Bottreau, A.-M.; Marzat, C.; Lacroix, Y.; Dutuit, Y. J. Microwave Power 1975, 10, 297.
(34) Bottreau, A.-M.; Dutuit, Y.; Marzat, C.; Moreau, J. Rev. Phys. Appl. 1976, 11, 163.
(35) Delbos, G.; Bottreau, A.-M.; Marzat, C.; Moreau, J. J. Microwave Power 1978, 13, 69.
(36) Schwan, H. P.; Sheppard, R. J.; Grant, E. H. J. Chem. Phys. 1976, 64, 2257.
(37) Szwarnowski, S.; Sheppard, R. J. J. Phys. E 1977, 10, 1163.
(38) Kaatze, U.; Giese, K. J. Phys. E 1980, 13, 133.
(39) Goulon, J. Final Report to the BCR Project 148; Community Bureau of Reference: Brussels, 1980.
(40) Van Loon, R.; Kestemont, E.; Finsy, R.; Bellemans, A. Final Report to the BCR Project 148; Community Bureau of Reference: Brussels, 1960.
(41) Blue, M. D. J. Geophys. Res. 1980, 85, 1101.
(42) Nightingale, N.R.V.; Szwarnowski, S.; Sheppard, R. J.; Grant, E. H. J. Phys. E 1981, 14, 156.
(43) Owen, B. B.; Miller, R. C.; Milner, C.F.; Cogan, H. L. J. Phys. Chem. 1961, 65, 2065.
(44) Vidulich, G. A.; Evans, D. F.; Kay, R. L. J. Phys. Chem. 1967, 71, 656.
(45) Kaatze, U. Chem. Phys. Lett. 1986, 132, 291.
(46) Debye, P. Polar Molecules; Chemical Catalog: New York, 1929.